Chapter 11

Label-Free Biosensors Based on Bimodal Waveguide (BiMW) Interferometers

Sonia Herranz*, Adrián Fernández Gavela*, and Laura M. Lechuga

Abstract

The bimodal waveguide (BiMW) sensor is a novel common path interferometric transducer based on the evanescent field detection principle, which in combination with a bio-recognition element allows the direct detection of biomolecular interactions in a label-free scheme. Due to its inherent high sensitivity it has great potential to become a powerful analytical tool for monitoring substances of interest in areas such as environmental control, medical diagnostics and food safety, among others. The BiMW sensor is fabricated using standard silicon-based technology allowing cost-effective production, and meeting the requirements of portability and disposability necessary for implementation in a point-of-care (POC) setting.

In this chapter we describe the design and fabrication of the BiMW transducer, as well as its application for bio-sensing purposes. We show as an example the biosensor capabilities two different applications: (1) the immunodetection of Irgarol 1051 biocide useful in the environmental field, and (2) the detection of human growth hormone as used in clinical diagnostics. The detection is performed in real time by monitoring changes in the intensity pattern of light exiting the BiMW transducer resulting from antigen–antibody interactions on the surface of the sensor.

Key words Bimodal waveguide interferometry, Evanescent field biosensor, Integrated optics, Immunoassay, Biofunctionalization, Biorecognition

1 Introduction

Most analytical methodologies used in fields such as environmental monitoring, medical diagnostics and food safety are based on time-consuming and expensive techniques that must be performed by specialized personnel in laboratory environments. This usually involves extensive time and effort due to the need for analysis and sampling, as well as interpretation of results. These can cause critical delays in clinical treatment decisions or removal of contaminated products from the market in order to avoid extended health

*These authors contributed equally to this work.

Avraham Rasooly and Ben Prickril (eds.), *Biosensors and Biodetection: Methods and Protocols Volume 1: Optical-Based Detectors*, Methods in Molecular Biology, vol. 1571, DOI 10.1007/978-1-4939-6848-0_11,

impacts. Therefore it is imperative to use reliable diagnostic tools that ensure sensitive, rapid, and simple analysis, and to expedite the diagnostic process.

In this context, biosensors are beginning to overcome the main drawbacks of classical analytical techniques. Modern biosensors are often portable, easy-to-use, and highly sensitive, and can operate in real-time and in-situ. Most of these photonic biosensors employ working principles and components (as waveguides) from the field of Integrated Optics (IO) (for basic information about IO, readers are referred to references [1, 2]). The IO-based biosensors are normally fabricated with standard Si-technology which employs well-known fabrication processes and silicon (Si) or silicon nitride (Si_3N_4) as core waveguide materials (*see* **Note 1**). Within IO-based biosensors, photonic interferometric biosensors based on the evanescent wave principle are highly suitable for many applications due to their high sensitivity and great potential to be integrated in a POC device [3].

1.1 Interferometric Sensors Based on Integrated Optics

The working principle of interferometric biosensor relies in the creation of an interference pattern, generated by the superposition of two or more light waves. In a common interferometric device, the incoming light beam is split in two beams of equal intensity that travel through different optical paths (arms) and are recombined before arriving at a detector, which collects the interferometric signal, as Fig. 1 shows.

For biosensing applications, one of the arms is used as a reference while the other acts as sensing one. Interferometric biosensors are based on the evanescent wave detection principle, therefore any modification in the sensing arm, such as binding events or concentration variation, induce a change of the effective refractive index of the guided light wave producing an interference pattern at the output.

The output intensity, $I(t)$, of an interferometric sensor is related with the phase difference between the two arms, $\Delta\varphi(t)$ as follows:

$$I(t) \propto \cos(\Delta\varphi)$$

$$\Delta\varphi(t) = \frac{2\pi L}{\lambda}\Delta n_{eff}$$

where L is the length of the sensing arm, λ the wavelength of the light, and Δn_{eff} the difference between the effective refractive index of the two propagated modes.

The phase difference, in an experimental interferometric signal, is determined by the variation between the initial value, $\Delta\varphi_1$, and the final value, $\Delta\varphi_2$, given by the number of fringes, where a complete fringe represents a phase difference of 2π, as Fig. 1 shows.

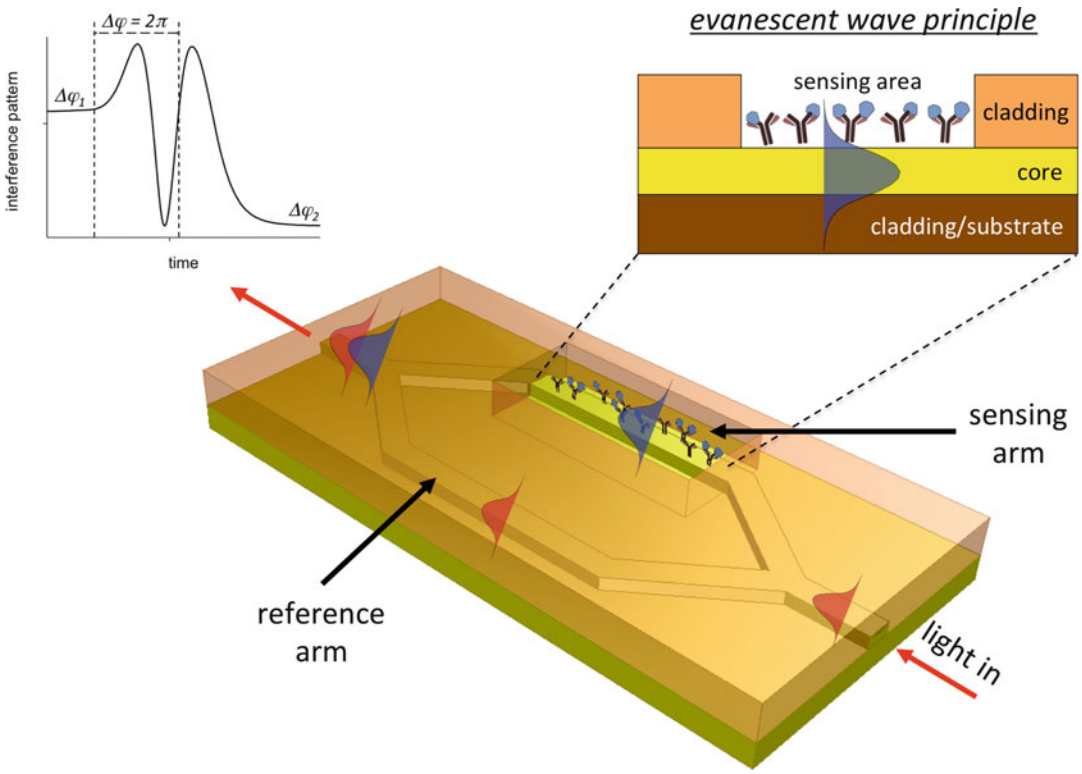

Fig. 1 Scheme of the working principle of an interferometric waveguide biosensor

Our work focuses on the development of IO nano-immunosensors based on BiMW transducers and their integration into a complete Lab-On-a-Chip (LOC) platform. BiMW is a novel interferometric transducer, which has been designed for sensitive, label-free, and direct detection of biomolecular interactions. In this IO interferometer, light is coupled in a straight single-mode rib waveguide, and after passing through a step-junction, two transversal modes with the same polarization are excited (*see* Fig. 2). Due to the presence of two propagated modes in a common path with different evanescent field profiles, any change in the refractive index causes an interference pattern at the device output. The intensity distribution at the output depends principally on the refractive index at the sensor surface, as well as on the dimensions of the BiMW structure (layers thicknesses and rib dimensions). The bimodal section of the BiMW includes a sensing window area free of cladding, in order to have access to the waveguide surface for sensing purpose (*see* Fig. 2), following the interferometric working principles explained previously. Therefore, by measuring the output light intensity the sensor response can be determined in a quantitative way [4].

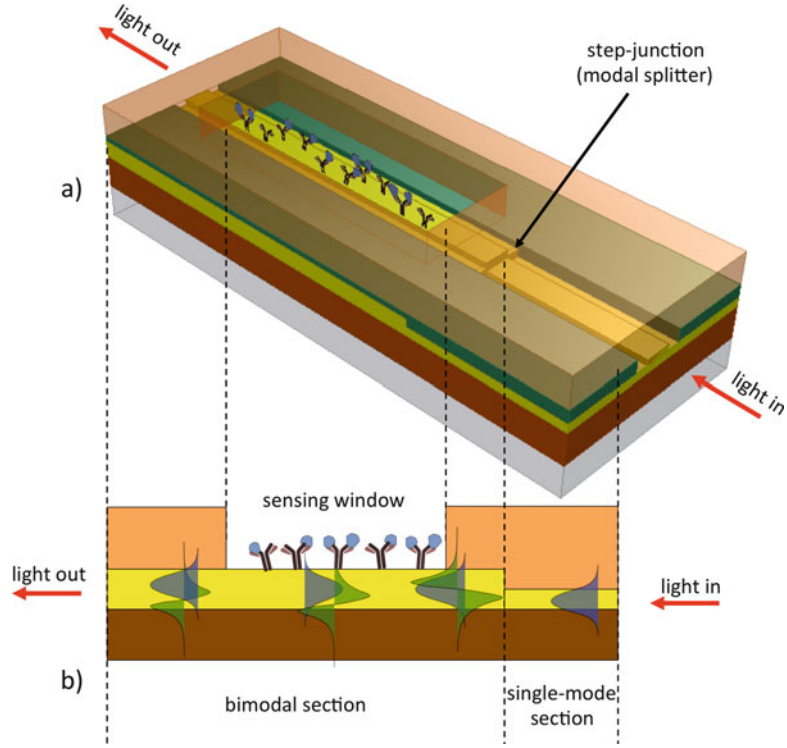

Fig. 2 (**a**) Scheme of a BiMW interferometric sensor. (**b**) Longitudinal side view of a BiMW showing the distribution of the electromagnetic field in several points

Interferometric sensors, and in particular BiMW interferometers, have proved to be one of the most sensitive devices for label-free analysis, reaching sensitivity to homogeneous changes in the refractive index of 10^{-7}–10^{-8} Refractive Index Unit (RIU), meaning that they have the potential to detect biomolecular interaction at pM levels. However, to use this technology for biosensing applications the transducer must be highly selective for instance, particularly with applications such as immunoassays (immunosensors). The limit of detection (LOD) achieved with an immunosensor is dependent not only on the transducer itself but also on the biorecognition element and the biofunctionalization protocol used to combine them.

Here we describe the design and fabrication process of BiMW interferometers, paying special attention to parameters affecting their performance (such as waveguide length or rib dimensions) in order to achieve the highest possible sensitivity. Additionally, we report the application of BiMW interferometry to biosensor development. Two applications in the fields of environmental monitoring and clinical diagnostics are described: the detection of Irgarol 1051 biocide and that of human growth hormone, respectively.

2 Materials

2.1 Equipment

1. Plasma cleaner reactor: Standard plasma system Femto, version A (40 kHz, 0–100 W) from Diener Electronic GmbH (Ebhausen, Germany).
2. Ultrasonic bath FB 15054, from Fisher Scientific (Madrid, Spain).
3. ABBE refractometer (Optic Ivymen System, Spain).
4. Clean Room facilities: the BiMWs are fabricated from a standard 4-in. (p-type) Si wafer with a thickness of 500 μm purchased from Siltronic Company. The fabrication of the BiMW is done at Clean Room facilities (class 100) using standard microelectronics optical photolithography, reactive ion etching, wet etching, and various deposition methods. Over the Si substrate a 2 μm thick layer of thermal oxide ($n_{\text{bottom,clad}} = 1.46$) is grown. Then, a 340 nm thick core layer of Si_3N_4 ($n_{\text{core}} = 2.00$) is deposited by Low Pressure Chemical Vapor Deposition (LPCVD). An absorbent layer of poly-crystalline Si ($n_{\text{poly}} = 4.06$) of 100 nm is deposited by LPCVD over a silicon dioxide (SiO_2) layer of 200 nm previously deposited. Finally, a SiO_2 ($n_{\text{top,clad}} = 1.46$) layer 1.5 μm thick is deposited by Plasma Enhanced Chemical Vapor Deposition (PECVD).

2.2 Setup Components

1. Fluid cell is made of polydimethylsiloxane (PDMS, Sylgard) fabricated using a methacrylate (PMMA) topographic master.
2. Syringe pump (NE300, New Era) for maintaining a constant flow during all the biochemical detection process.
3. An injection valve (V-451, Idex) allows the injection of different solutions without changing the flow rate.
4. Laser diode (ML101J27, Mitsubishi) with $\lambda_0 = 660$ nm and $P = 120$ mW, mounted on a compact temperature controlled laser diode mount (TCLDM9, Thorlabs), is used as light source. A Temperature controller (TED 200C, Thorlabs) and current controller (LDC220C, Thorlabs) are employed to stabilize the laser diode.
5. To couple the light into the waveguide a lenses system is used, composed by: collimated lens (C240TME-D, Thorlabs), polarization-dependent isolator (IO-3D-660-VLP, Thorlabs) and coupling objective 40× (Achro, Leica).
6. A four quadrants photodetector (S4349, Hamamatsu) is employed for collecting the light at the end of the device. The signals are amplified through standard benchtop instrumentation (PDA200C, Thorlabs).

7. A digital acquisition card (6251, National instruments) for reading the photodetector signal in real time. The signal acquisition is controlled by a LabVIEW-based application.
8. 3-axis precision micro-position stage (Nanomax-TS, Thorlabs) is used for laser-BiMW alignment.
9. A temperature sensor (AD590, Thorlabs) is used to achieve a temperature feedback circuit together with a thermo-electric cooler (TEC3-1.5, Thorlabs), operated through a bench top temperature controller (TED200C, Thorlabs) allowing a temperature resolution of 0.01 °C.

2.3 Reagents

1. Potassium phosphate monobasic (KH_2PO_4, P0662-500G), sodium phosphate dibasic (Na_2HPO_4, S0876-500G), sodium chloride (NaCl, S9625-1KG-D), potassium chloride (KCl, 60,128-250G-F), 2-(N-Morpholino)ethanesulfonic acid (MES, M3671-50G), sodium carbonate (Na_2CO_3, S7795-500G), sodium hydroxide (NaOH, S8045-500G), sodium dodecyl sulfate (SDS, 436,143-25G), hexadecyltrimethylammonium bromide (CTAB, H6269-100G), bovine serum albumin (BSA, A7906-10G), (3-aminopropyl)triethoxysilane (APTES, A3648-100ML), *N*-hydroxysulfosuccinimide sodium salt (sulfo-NHS, 56,485-1G), *N*-(3-dimethylaminopropyl)-*N*-ethylcarbodiimide hydrochloride (EDC, E1769-1G, *see* **Note 2**), *N*,*N*-dimethylformamide anhydrous (DMF, 227,056-100ML), toluene (244511-1 L), pyridine (270970-100ML), *p*-phenylene diisothiocyanate (PDITC, 258,555-5G), hydrofluoric acid (HF, 695,068-25ML-D), ammonium fluoride (NH_4F, 338,869-25G), and phosphoric acid (85 wt. % in H_2O, W290017-1KG-K) can be purchased from Sigma-Aldrich.
2. Acetone (161007.1211), ethanol absolute (161086.1211), methanol (161091.1211), nitric acid (65%, 473255.1611), and hydrochloric acid (HCl 37%, 471020.1611) can be purchased from Panreac.
3. Recombinant human Growth Hormone (r-hGH, 22 kDa) was provided by Dr. Parlow (National Hormone and Peptide Program (NHPP), National Institute of Diabetes and Digestive and Kidney Diseases (NIDDK), CA, USA). The monoclonal antibody (anti-hGH) was produced and characterized at the Department of Immunology and Oncology from the National Center of Biotechnology (CNB-CSIC, Madrid, Spain) [5].
4. Irgarol 1051, Irgarol 1051 derivative *4e* (hapten) [6], and anti-Irgarol 1051 serum (As87) were provided by Prof. Marco (Nanobiotechnology for Diagnostics Nb4D group, IQAC-CSIC, Barcelona, Spain).
5. Deionized water from a Milli-DI® Water Purification System, Merck Millipore, USA.

2.4 Buffer Composition

1. Buffered hydrofluoric acid (BHF): mixture of HF and NH_4F, 1:6 (v/v)
2. MES buffer: solution of 0.1 M MES and 0.5 M NaCl in water, pH adjusted to 5.5. Store at 4 °C.
3. Phosphate buffer saline (PBS): solution of 137 mM NaCl, 2.7 mM KCl, 8 mM Na_2HPO_4, and 2 mM KH_2PO_4 in water, pH adjusted to 7.4. Store at 4 °C. We recommend preparing a ten-fold concentration PBS (10× PBS, pH 7–7.5) as stock solution, which can be stored at room temperature (RT). Then, prepare a working solution of 1× PBS by dilution from the stock solution. Alternatively, PBS can be purchased from Sigma-Aldrich (P7059-1 L).
4. Carbonate buffer (CB): 0.1 M Na_2CO_3 at pH 9.

3 Methods

One of the first steps to develop a BiMW transducer of high sensitivity is to simulate a range of different core and cladding thicknesses, taking into account the rib dimensions and the tolerances at the clean room facilities where the fabrication will be done. The sensitivity of an interferometry-based transducer is directly related with the dimension of the interaction surface (*see* Subheading 1.1), thus higher sensitivity is obtained with a long sensing area. For that reason a compromise between the total length of the BiMW chip and the quantity of devices per wafer needs to be reached, for a cost-effective fabrication.

Once the optimum dimensions have been defined by modelling, lithographic masks are designed according the chosen dimensions and then the BiMW devices are fabricated at clean room facilities. The fabrication processes should be reproducible and must guarantee the same reliable performance for all the BiMW transducers.

To characterize the device, BiMW is placed in a custom-designed setup. The light from a laser diode is end-fire coupled using a lens system, as Fig. 3 shows. For light readout, a two-section photodetector is employed as the interference of the common path BiMW interferometer generates a variation of the output intensity distribution, but the total intensity should be constant. The photodetector must be placed directly at the BiMW output, and total intensity must be divided in the up and down quadrant of the photodetector (*see* Fig. 3). The sensor response, S_R, is determined through the equation:

$$S_R = \frac{I_{up} - I_{down}}{I_{up} + I_{down}}$$

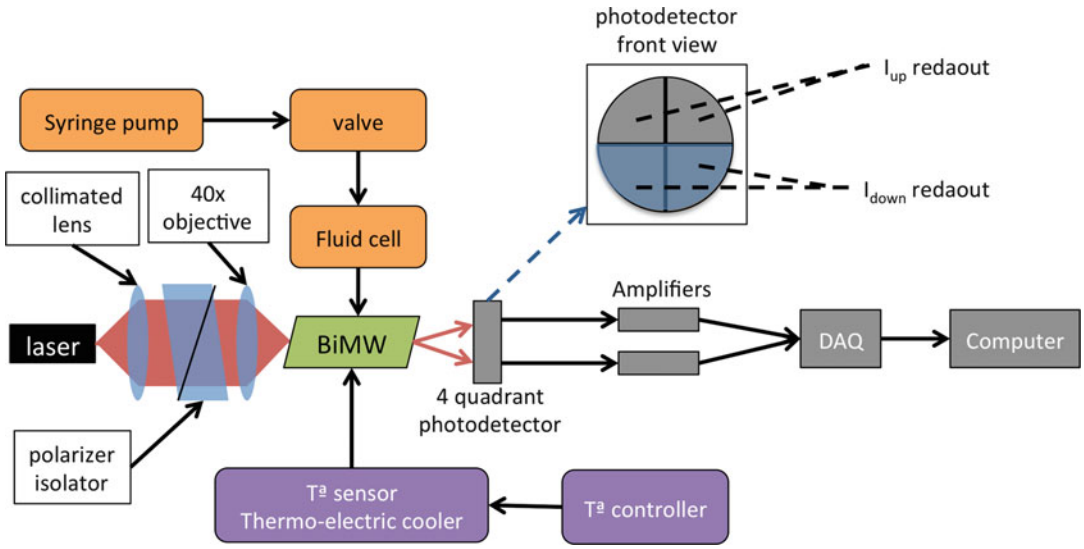

Fig. 3 Scheme of the experimental setup employed for the evaluation of the BiMW sensors

where I_{up} and I_{down} are the intensities acquired for the up and down quadrants of the photodetector, respectively.

For the application of the BiMW interferometer as a biosensor the surface must be modified with a recognition element or biological receptor which, when immobilized onto the surface, increases the transducer selectivity for the substance to be monitored. The environmental and clinical diagnostic BiMW interferometric biosensor applications will be illustrated.

Irgarol 1051 is a protective algaecide (biocide, s-triazine compound) used in antifouling paints to prevent attachment and growth of biofouling organisms in the aquatic environment. It leaks out from the paint and by its toxicity Irgarol 1051 prevents accumulation of organisms onto the painted surface (boat hulls or marine installations). Traces of Irgarol 1051 have been detected in the marine environment [7, 8], and due to its broad toxicity (photosystem-II inhibitor), Irgarol 1051 is potentially toxic toward valuable aquatic species (mainly small aquatic plants), and its presence in the environment can cause significant environmental problems. In fact, a number of studies have demonstrated its negative impact on marine organisms such as corals.

Human growth hormone (hGH) is produced by the pituitary gland and promotes growth, regulates the activity of vital organs and helps to preserve the health of the whole organism. Its deficiency commonly affects children and has several negative effects such as hypoglycemia in newborn infants or stunted growth in children. hGH deficiency is results from several genetic diseases such as Turner syndrome and Prader-Willi syndrome. Thus the hGH level in blood or urine can be used for the diagnosis of

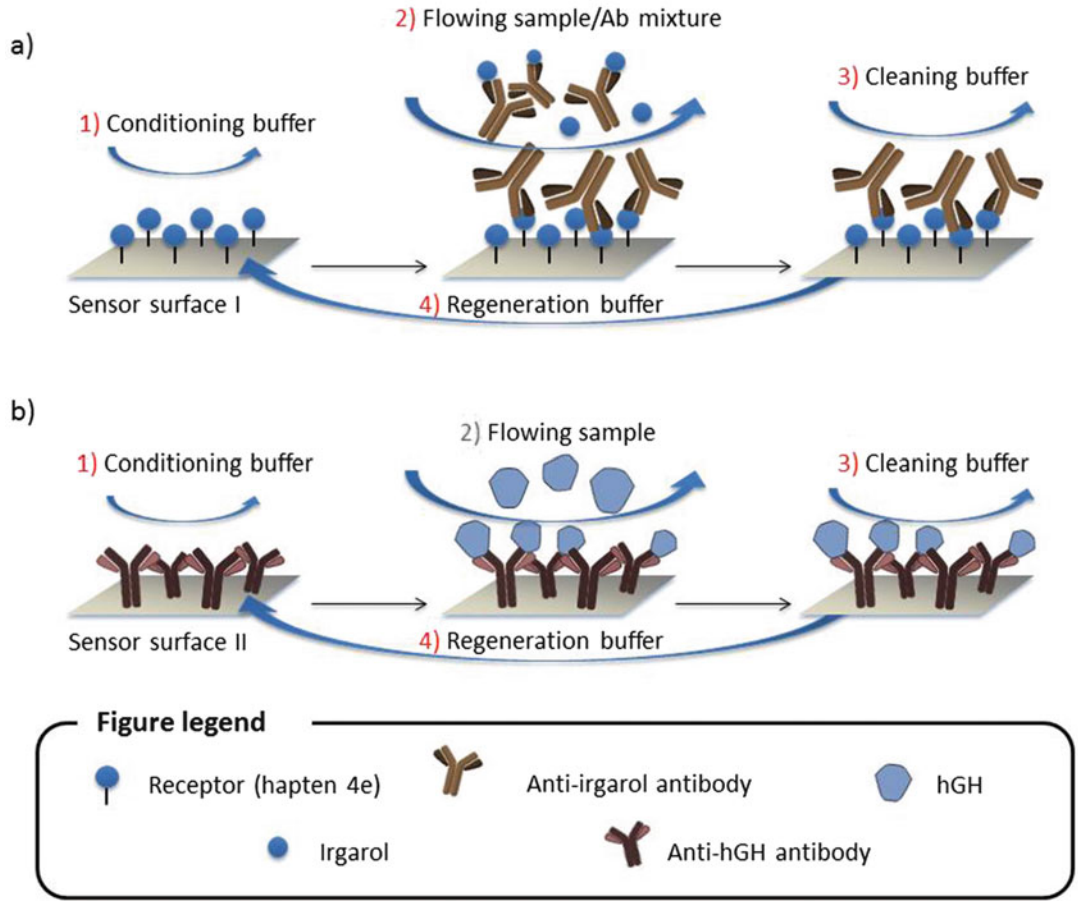

Fig. 4 Immunoassay formats: (**a**) Competitive immunoassay format selected for Irgarol 1051 detection (**b**) Direct immunoassay format selected for hGH detection. For sensor surface details, *see* Fig. 7

those disorders. Additionally, r-hGH has been used by many sportsmen in an attempt to improve athletic performance, and the control of hGH level in urine is usually employed as a doping test.

Both biosensor applications are based on antigen–antibody specific interactions. For the analysis of Irgarol 1051, a low molecular weight pollutant, a competition immunoassay has been selected (*see* Fig. 4a). The transducer surface is functionalized with an Irgarol 1051 derivative (hapten *4e*). A fixed amount of an anti-Irgarol antibody is mixed and allowed to interact with the sample and then, the mixture is injected to the flow cell where the sensor is placed. The free antibodies interact with the immobilized *4e* receptor and generate a binding response, which is inversely related to the concentration of Irgarol 1051 in the sample (*see* Fig. 5a). The detection of hGH is carried out by using a direct immunoassay (*see* Fig. 4b). In this case the transducer surface is functionalized with an anti-hGH antibody. The hGH present in the

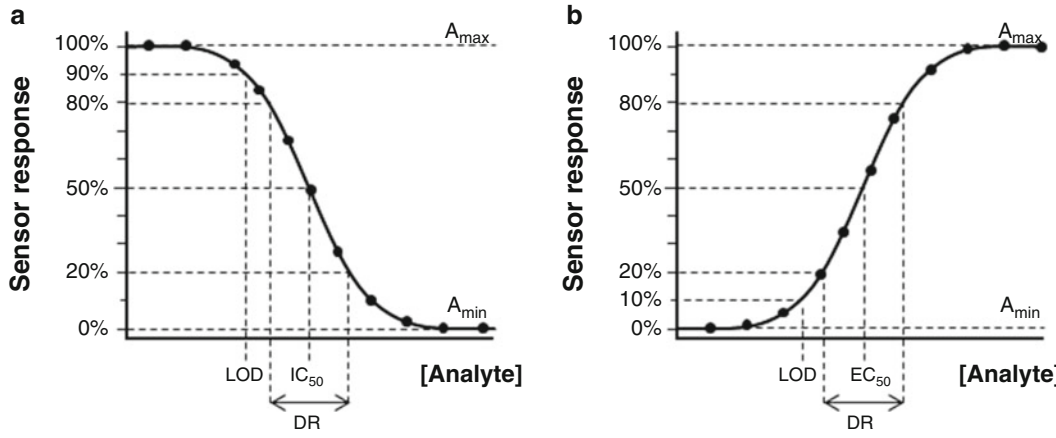

Fig. 5 Standard calibration curves showing the relationship between the analyte concentration ([Analyte], logarithmic scale) and the sensor response for: (**a**) competitive and (**b**) direct immunoassays

Table 1
Layer parameters employed for the evaluation of the single-mode and bimodal condition

Layer	Material	Thickness (nm)	Refractive index
Top cladding	Water/SiO_2	1500	1.33/1.46
Core	Si_3N_4	150–340	2.00
Bottom cladding	SiO_2	2000	1.46

injected sample interacts with the immobilized antibody and generates a binding response directly related to its concentration (*see* Fig. 5b).

3.1 BiMW Simulation and Fabrication

3.1.1 BiMW Simulation

(a) To design a BiMW we need to choose optimal materials, which ensure a cost-effective fabrication, a further integration onto a complete LOC platform, and a highly sensitive device. As the transducers are designed for biosensors applications, $SiO_2/Si_3N_4/SiO_2$ waveguides are selected [9]. Table 1 summarizes the parameters employed in the calculation, relative to the materials' refractive indices and their thicknesses.

(b) Once the material is defined, core dimensions are analyzed to ensure the best sensitivity of the device. For that, different considerations have to be taken into account [4] (*see* Fig. 6):

- Single-mode behavior (mode TE_{00} or TM_{00}) in section A in Fig. 6b.
- Bimodal behavior (mode TE_{00} and TE_{10} or TM_{00} and TM_{10}) in sections B, C, and D in Fig. 6b.
- Performances achievable in the clean room facilities.

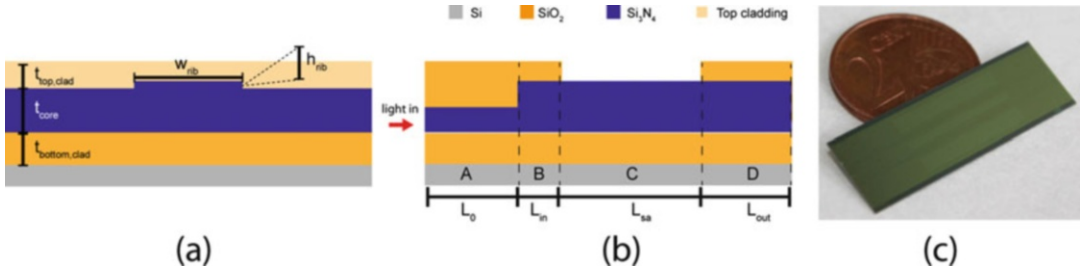

Fig. 6 (**a**) Front cross section of the employed rib-waveguide, indicating the main parameters described on the text. (**b**) Longitudinal side view of the BiMW device. Light is injected in the single-mode section (A). After an abrupt step junction, two modes propagate till the end of the device. Regions B and D are covered by silicon dioxide while C is exposed to the external medium (sensing area). (**c**) Picture of a chip with 20 BiMW sensors

Table 2
Optimal parameters for core dimensions in a high sensitivity BiMW

Section	t_{core} (nm)	h_{rib} (nm)	w_{rib} (nm)
Single-mode	150	1.5	3000
Bimodal	340	1.5	3000

In bimodal section, bulk and surface sensitivity must be calculated for different core thicknesses (t_{core}). Once t_{core} has been fixed, the thickness of the single-mode section is chosen to determine how the energy carried by the fundamental mode, propagating in section A in Fig. 6b, is distributed to the two modes propagating in section B in Fig. 6b.

Table 2 summarizes the optimal parameters for core dimensions in a BiMW for a $\lambda = 660$ nm and TE polarization (*see* Fig. 6a).

(c) Once the core dimensions are defined, the sensor design is completed by choosing the length of the different sections. It is required to take into account the following considerations:

- The need to adapt a microfluidic system to the BiMW for biosensing applications.
- To ensure high sensitivity while keeping a reasonable total length.
- Distribution of the BiMWs in 4-in. silicon wafer to optimize cost-effective fabrication.

The following values were chosen: $L_0 = 3$ mm, $L_{in} = 4.5$ mm, $L_{sa} = 15$ mm, and $L_{out} = 8.5$ mm (*see* Fig. 6b).

(d) In a 4-in. silicon wafer, 240 BiMW are distributed in 12 different chips (1 cm wide × 3.1 cm long) with 20 sensors per chip (*see* Fig. 6c).

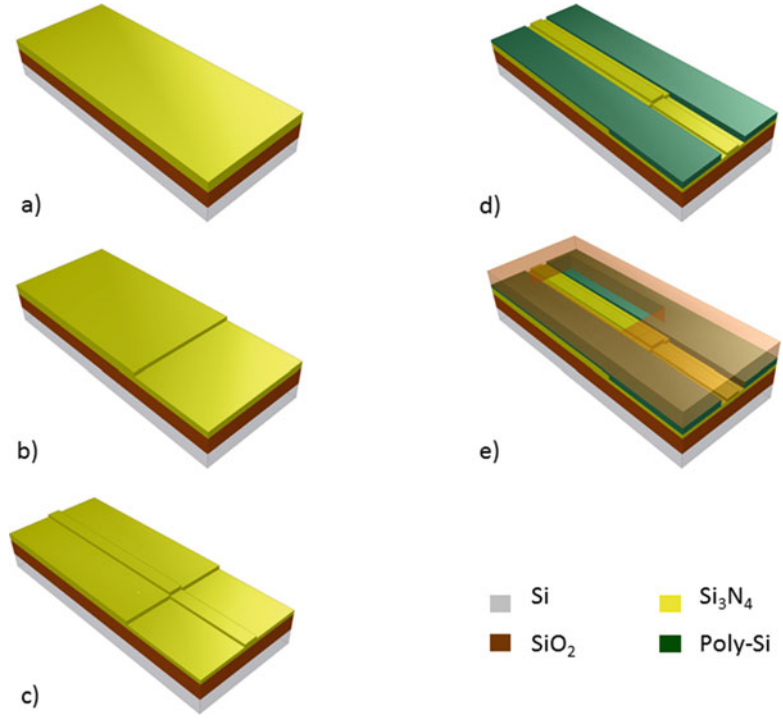

Fig. 7 Scheme of the fabrication process of integrated BiMW sensors. (**a**) A layer of SiO_2 and Si_3N_4 is deposited on a Si wafer. (**b**) Step-junction etched in Si_3N_4 layer for single-mode section definition. (**c**) Rib structure is defined. (**d**) Polycrystalline deposition over the Si_3N_4 and etching process to open desired window on this layer. (**e**) SiO_2 deposition and sensing area opening

3.1.2 *BiMW Fabrication*

Figure 7 summarizes the fabrication process. Below, each step of Fig. 7 is explained.

(a) The fabrication processing starts with a 4-in. (p-type) Si wafer with a thickness of 500 μm, over which a 2 μm thick layer of thermal oxide is grown. Then a 340 nm thick core layer of Si_3N_4 is deposited by LPCVD.

(b) The thickness of the Si_3N_4 is reduced 190 nm to obtain a 150 nm single-mode section using a wet etching process with 75% phosphoric acid at 160 °C. A hard mask constituted by a layer of SiO_2 deposited by PECVD and defined by photolithography is employed in this step to protect unexposed regions.

(c) Using a wet etching process with BHF and a standard photolithography process, the rib structure of the waveguide (3 μm in width and 1.5 nm in height) is defined. The low

etching rate of the BHF for Si_3N_4 allows precise control of the process.

(d) A 100 nm layer of poly-crystalline Si is grown by LPCVD over 200 nm of SiO_2 deposited by PECVD, which is introduced to improve the adhesion to the underlying Si_3N_4 surface. A standard lithography process is used to define the structure. Dry etching (RIE) is employed to remove the poly-crystalline Si layer and 150 nm of silicon dioxide, to ensure vertical sidewalls. Then, a wet etching process is used to eliminate the remaining 50 nm of SiO_2. Poly-crystalline Si layer is employed as absorbing material to define lateral bands along the waveguide path.

(e) A SiO_2 layer 1.5 μm thick is deposited by PECVD as top cladding layer. In order to open the sensing area a standard lithography process is done, employing a wet etching process with BFH to remove the desired SiO_2.

3.2 Setup Configuration

(a) The BiMW chip is placed in an aluminum homemade holder as shown in Fig. 8. Into the holder a temperature stabilization is included, and the entire system is mounted on a 3-axis stage. In this way, it is possible to focus the light in the desired BiMW sensor optimally.

(b) As the total output intensity must be divided in the up and down quadrant of the photodetector, this one is joined in a 2-axis stage assembly to the aluminum chip holder, to ensure the right position of the photodetector at the BiMW

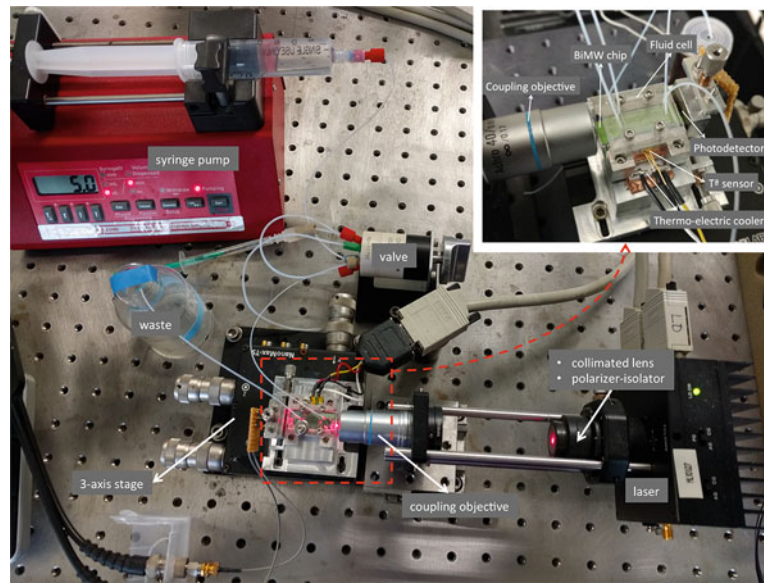

Fig. 8 Photograph of a BiMW experimental setup

output. As photodetector has four quadrants, two BiMW could be measure simultaneously, using two quadrants per sensor. This position is essential if a modulated signal is required [10].

(c) A digital acquisition card connected to a computer is employed to process the photodetector signal. A homemade Labview software acquires a continuous photodetector signal in real time.

(d) A diode laser is placed in a temperature controlled mount. To guarantee an optimal end-fire incoupling of the laser beam, a lenses system is employed. A lens is used to collimate the divergent laser beam of the diode. After this lens a polarization-dependent isolator is placed to avoid optical back reflections and to guarantee the required polarization. Finally, a 40x objective is employed to focus the collimated beam to the BiMW input for end-fire coupling.

(e) All the biological interactions must be performed in a liquid medium. For that reason, a PDMS fluid cell must be placed on top of the sensor chip. This fluid cell has channels of 11 µL volume, and an inlet and outlet for liquid flow. To avoid liquid leaks between the PDMS channels and the BiMW chip, and in order to properly align the fluid cell, four screws and a methacrylate sheet are employed to press, as Fig. 9 shows.

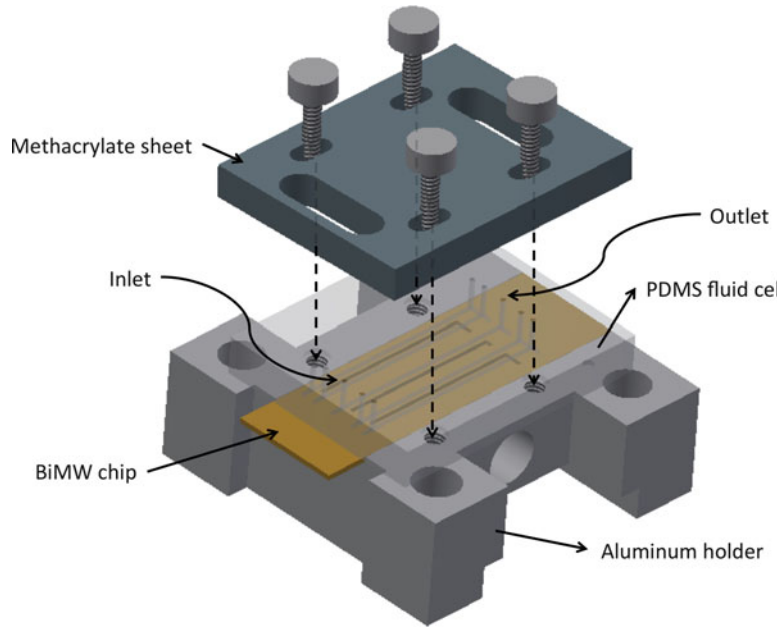

Fig. 9 Scheme of the fluidic cell employed for BiMW evaluation

(f) The flow delivery system is mounted by connecting a syringe pump with an injection valve and this one to the cell flow inlet by using Teflon tubes. The length of the tubes should be reduced as much as possible to minimize diffusion effects. The loop of the injection valve has a variable length, depending on the desired volume. Here, 150 μL and 250 μL loops have been used for Irgarol 1051 and hGH immunoassays, respectively. An extra tube is used from the cell outlet to the waste.

3.3 Sensing Characterization: Homogeneous Sensing

1. The determination of the BiMW biosensor bulk sensitivity allows evaluating the response of the transducer, independently of the biofunctionalization process. For that, milli-Q water is supplied to the sensor in a continuous rate (40 μL/min), and solutions providing small refractive index changes, such as different concentrations of HCl are injected over the sensor.
2. Previously to the injections, the refractive index of the solutions is checked with a commercial refractometer, and the difference of refractive index, Δn, between the continuous buffer running and the injected solutions is calculated.
3. Taking into account the sinusoidal relationship between the phase change, $\Delta\varphi$, and the output intensity, I, in an interferometric device [3], changes of the refractive indexes over the sensor area, induce output signal alterations through the evanescent field interaction.
4. Phase variation, $\Delta\varphi$, is plotted versus index variation, Δn, obtaining a calibration curve as Fig. 10 shows. The slope of the fitting curve, expressed in rad/RIU, represents the bulk sensitivity of the sensors. For BiMW, the sensitivity (S_{bulk}) is around $1700 \cdot 2\pi$ rad/RIU, for TE polarization.
5. The LOD, Δn_{min}, is calculated through the equation:

$$\Delta n_{\text{min}} = \frac{\Delta\varphi_{\text{min}}}{S_{\text{bulk}}} = \frac{\Delta S_{\text{R,min}}}{S_{\text{bulk}}}\frac{\pi}{V} = \frac{3 \cdot \sigma_{S_{\text{R}}}}{S_{\text{bulk}}}\frac{\pi}{V}$$

where $S_{\text{R,min}}$ is the minimum sensor response, defined as three times the system noise, $\sigma_{S_{\text{R}}}$. V is the visibility of the output signal, which corresponds to π rad in the phase variation. LOD for BiMW sensors are in the range of 10^{-7}–10^{-8} RIU.

3.4 Surface Biofunctionalization

The most widely applied approaches to chemical modification of Si_3N_4 surfaces are based on the molecular grafting of the native oxide layer present onto this material by forming self-assembled monolayer (SAM) of alkyl-silanes. Among the wide variety of commercially available silanes, APTES ((3-aminopropyl)triethoxysilane) is one of the most employed for chemical modification of Si-based photonic devices. Surfaces modified with APTES present

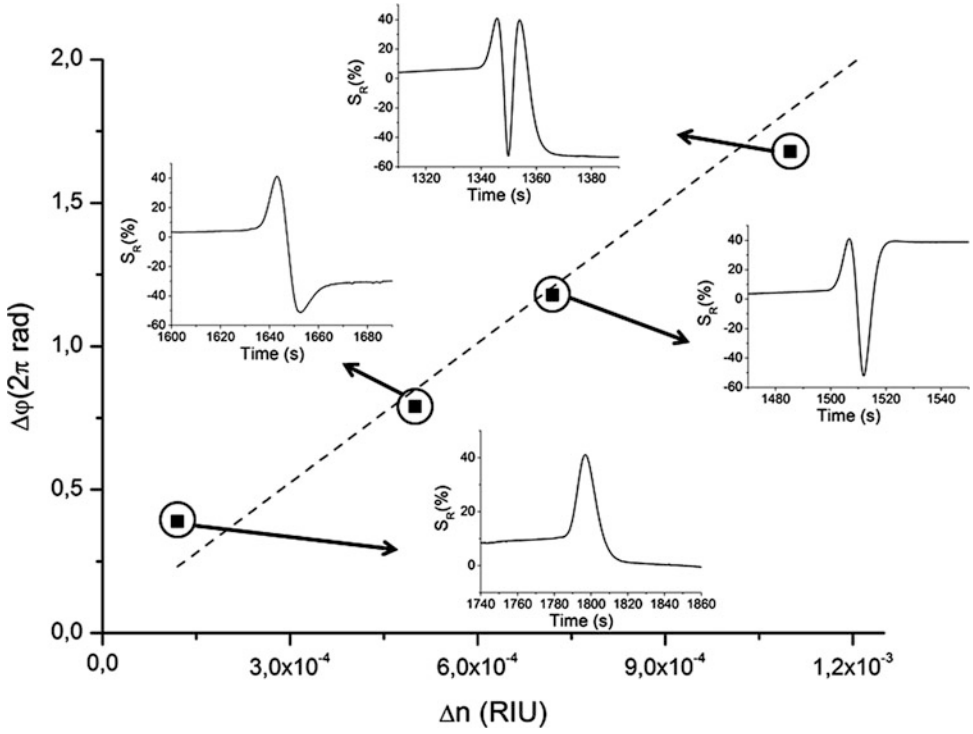

Fig. 10 Calibration curve for a BiMW sensor. Insets represent the temporal interferometric signals corresponding to the entrance of solutions with different refractive indexes

3-aminopropyl moieties, which allow the further covalent immobilization of bioreceptors presenting carboxyl groups in their structure. Moreover, by using different cross-linker molecules, the variety of bioreceptors that can be covalently attached is multiplied.

We describe the use of APTES to chemically modify the BiMW chips. APTES-modified chips are then functionalized by covalently attaching the hapten *4e*, resulting in a biosensor surface which can detect Irgarol 1051 by a competitive immunoassay (Surface I). In the second approach, APTES-modified chips are biofunctionalized by covalently attaching the anti-hGH antibody, using *p*-phenylene diisothiocyanate (PDITC) as a cross-linker molecule (Surface II). PDITC displays two isothiocyanate groups, which can couple the free amine groups of a bioreceptor. Additionally, PDITC has the potential to form well-organized assemblies driven by π–π stacking, resulting in improved antifouling properties [11]. Surface II is used to detect hGH by a direct immunoassay.

In order to avoid contamination of the surface and to enhance silanization efficiency and reproducibility, the BiMW chips are thoroughly cleaned and oxidized forming a fresh prepared oxide layer with a high density of silanol groups (reactive hydroxyl groups). This procedure is carried out immediately prior to the

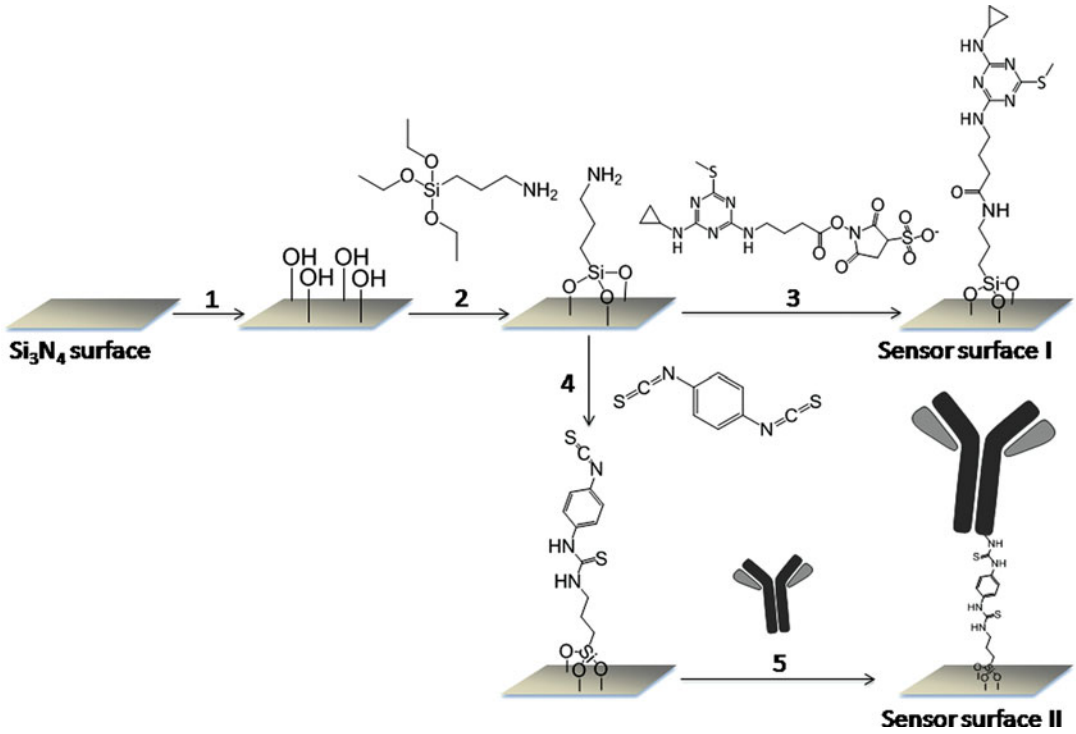

Fig. 11 Functionalization scheme/protocol: (*1*) cleaning and oxidation; (*2*) APTES silanization; (*3*) covalent attachment of hapten 4e; (*4*) activation of APTES-modified surface with PDITC, and (*5*) covalent attachment of anti-hGH antibody. Sensor surface I: 4e-functionalized surface, used for Irgarol 1051 immunodetection. Sensor surface II: anti-hGH antibody-functionalized surface, used for hGH immunodetection

surface biofunctionalization. Avoid storage of cleaned and oxidized chips, which are susceptible to contamination.

Figure 11 shows a scheme of the different steps of the functionalization protocol. Briefly, the BiMW chips are cleaned, oxidized (Fig. 11, step 1), and immediately silanized with APTES (Fig. 11, step 2). Then, sulfo-NHS-ester activated *4e* hapten is covalently attached (Fig. 11, step 3) getting sensor surface I. For preparing sensor surface II, APTES-modified chips are activated with PDITC (Fig. 11, step 4) and finally anti-hGH antibody is covalently bound (Fig. 11, step 5).

3.4.1 *Cleaning Procedure*

(a) Wipe the BiMW chip down using a cleanroom paper soaked in acetone.

(b) Sequentially rinse the chip with acetone, ethanol, and deionized water, and dry under nitrogen flow.

(c) Immerse the chip in 1% SDS aqueous solution and sonicate for 5 min.

(d) Rinse the chip with deionized water and dry again under nitrogen flow.

(e) Immerse the chip in a mixture of methanol and 37% fuming hydrochloric acid (1:1, v/v) and sonicate for 10 min (*see* **Note 3**).

(f) Finally, generously rinse the chip with deionized water and dry carefully under nitrogen flow.

3.4.2 Oxidation Procedure

(a) Treat the cleaned BiMW chip with oxygen plasma (100 W, 45 sccm) for 5 min (*see* **Note 4**).

(b) Immerse the chip in 15% HNO_3 at 75 °C for 25 min.

(c) Rinse generously the chip with deionized water, dry carefully under nitrogen flow and immediately immerse it in the silanization solution.

3.4.3 BiMW Interferometer Silanization Procedure Using APTES

(a) Clean and oxidize the BiMW chip according to the previous sections.

(b) Immediately immerse the BiMW chip in a solution of 1% APTES and incubate at RT for 1 h. Two different solvents have been evaluated: absolute ethanol and toluene.

(c) Amply rinse the chip with the silanization solvent and deionized water, sequentially.

(d) Dry the chip thoroughly under nitrogen flow and thermally treat it in an oven at 110 °C for 1 h.

3.4.4 Covalent Immobilization of Irgarol Derivative "4e"

(a) At this point, an APTES-modified BiMW (silanization solvent: toluene) chip is positioned on the experimental apparatus, and a PDMS multichannel gasket (flow-chamber) is pressed against it, forming the assay flow channels (*see* Fig. 9). The immobilization of the Irgarol derivative *4e* is carried out inside the measuring setup, using a *stopped-flow* incubation approach, i.e., by filling the flow channel with the reaction mixture and stopping the flow. After the appropriate incubation time, the reaction is stopped by restarting the flow and washing out the surface with deionized water.

(b) Prepare a solution mix of hapten *4e*, EDC, and sulfo-NHS in MES buffer. Concentrations must be optimized for each application; however, concentration typically ranges from 10 to 50 μg/mL of hapten, and 0.2–0.4 M and 0.05–0.1 M of EDC and sulfo-NHS, respectively. Pre-incubate this mixture for 30 min to 4 h at room temperature (amine-reactive sulfo-NHS ester hapten intermediate solution).

(c) Initiate a continuous flow (20 μL/min) of deionized water and wait until stabilization of the interferometric signal.

(d) Inject into the flow cell a volume of the NHS-activate *4e* solution large enough to fill the whole assay flow channel (25–50 μL). Once the channel is filled up, stop the flow and incubate from 4 h to overnight.

(e) Remove the NHS-activate *4e* solution by flushing deionized water through the flow channel for 5 min.

(f) BiMW chip is now functionalized and ready to be used for Irgarol 1051 immunodetection.

3.4.5 Covalent Immobilization of Anti-hGH Antibody

(a) Prior to the covalent attachment of the anti-hGH antibody, the APTES-modified chip (silanization solvent: ethanol) must be activated with PDITC, which acts as cross-linker. After PDITC activation the antibody can be immobilized through the amine groups present in its structure.

(b) Prepare a 20 mM PDITC solution (5 mL) in anhydrous DMF containing 1% pyridine.

(c) Immerse the APTES-modified chip in PDITC solution and incubate in the dark for 2 h.

(d) Wash off unbound reagents by sequentially rinsing the chip with acetone, ethanol and water, and dry it under nitrogen stream.

(e) Add 50–100 μL of a solution of anti-hGH antibody in carbonate buffer onto the PDITC-modified chip, cover it with a coverslip and incubate overnight, in the dark. Concentrations must be optimized for each application. For hGH immunoassay, a 50 μg/mL solution was used.

(f) Rinse the functionalized chip with PBS and carefully dry it under nitrogen stream.

(g) At this point, the functionalized BiMW chip is positioned on the experimental apparatus and the PDMS flow-chamber mounted. Before starting sample evaluation the sensor surface is blocked to avoid nonspecific adsorption and reduce background signal (*see* **Note 5**).

(h) Initiate a continuous flow of PBS and wait until the interferometric signal stabilizes.

(i) Inject into the flow cell a 2 mg/mL BSA solution in PBS until the flow channel is full. Then stop the flow and incubate for 1 h (*see* **Note 6**).

(j) The BiMW chip is now functionalized and ready to begin the sample evaluation. If not used immediately chips must be dried and stored at 4 °C. Before use, the chip is positioned again on the experimental apparatus and the sensor surface is conditioning by maintain a continuous flow of PBS for 1 h.

3.5 Detection by a Competitive Immunoassay

3.5.1 Selection of the Antibody Concentration

(a) Initiate a continuous flow of PBS and wait until stabilization of the interferometric signal. This buffer will be used to perform the Irgarol 1051 immunodetection assay.

(b) Prepare series of solutions (300 μL) with different dilution factors of the antibody (serum As87). For Irgarol 1051 detection, dilutions ranging from 1:10,000 to 1:500 were used.

(c) Inject into the flow cell the antiserum solutions with a regeneration step in between, and measure the phase shift (sensor response). Regeneration consists in disrupting the receptor–antibody interaction while maintaining the receptor onto the surface with minimal damage, by washing up the sensor surface with the so-called regeneration solution. Regeneration solution composition must be empirically optimized (*see* **Note 7**). For Irgarol 1051 immunoassay, a 50 mM NaOH solution was employed.

(d) Construct a plot of sensor response vs. antiserum concentration. Choose an antibody concentration value (fixed concentration to perform the inhibition assay) below the saturation limit, able to give high enough response intensity (phase shift), so that at inhibition, signals would be still clear. Take into account that by decreasing the antibody concentration, a better limit of detection can be achieved (*see* **Note 8**).

3.5.2 Detection of Irgarol 1051

(a) Initiate a continuous flow of PBS (20 μL/min) and wait until the interferometric signal is stabilized.

(b) Prepare a series of solutions of different concentrations of Irgarol 1051 in PBS (300 μL, standard solutions). Concentrations of the standard solutions to be measure depend on the limit of detection for each specific application. For Irgarol 1051, the standard solutions were in the ng/L to μg/L range.

(c) Mix the series of standard solutions with a volume of As87 serum so that the final dilution factor in solution equals that previously selected. Incubate the mixture for 10 min.

(d) Pump one antibody-Irgarol standard solution into the flow cell at 20 μL/min. This step produces a shift phase of the wave ($\Delta\varphi$) due to the interaction of the free antibody with the immobilized antigen.

(e) Wash off the unbound antibody by pumping PBS for a few minutes (20 μL/min).

(f) Regenerate the surface by injecting 50 mM NaOH (20 μL/min, 120 s), and wait until stabilization of the signal (surface conditioning). At this point, the surface is ready for the measurement of a second standard solution. In Fig. 12,

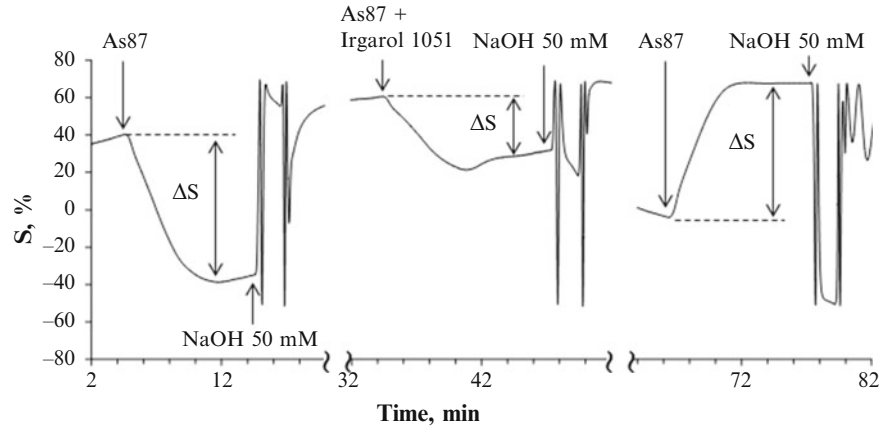

Fig. 12 Real monitoring of anti-Irgarol 1051 antibody (As87) detection. The presence of Irgarol 1051 (1 μg/L) in solution leads to a decrease of the sensor response. The sensor surface was regenerated with 50 mM NaOH

the sensor response for three consecutively samples (in PBS) is represented, in which the inhibition of the signal by the presence of Irgarol 1051 in the sample can be noticed.

(g) Construct a plot of sensor response vs. Irgarol 1051 concentration and fit the data to an appropriate curve-fitting model for obtaining the calibration curve (*see* **Note 9**). Limit of detection (LOD) should be in the desired range for the application. If not, try to optimize immobilization and immunoassay conditions. Irgarol 1051 levels typically range from 0.1–1.7 μg/L in marinas and 1–40 ng/L in coastal and estuarine waters [12], so a LOD at low ng–pg/L level is desirable.

(h) Mix the Irgarol samples (unknown concentrations) with an equal concentration of anti-Irgarol serum used with the standard solutions. Incubate the mixture for 10 min.

(i) Pump the antibody-sample mixture into the flow cell at 20 μL/min. After monitoring the antigen–antibody interaction, regenerate and condition the sensor surface in order to prepare it for the next analysis.

(j) The concentration of Irgarol 1051 in the measured samples can be estimated by interpolating the sensor response in the fitting curve.

3.6 Detection of hGH by a Direct Immunoassay

1. Initiate a continuous flow of PBS and wait until the signal is stabilized.
2. Prepare a series of solutions of different concentrations of hGH in PBS (400 μL, standard solutions). For hGH, the standard solutions were in the ng/L to μg/L range.

3. Inject into the flow cell the hGH solutions with a regeneration step in between (regeneration solution: 20 mM HCl), and measure the phase shift (sensor response).
4. Construct a plot of sensor response vs. hGH concentration and fit the data to an appropriate curve-fitting model for obtaining the calibration curve. The hormone hGH usually appears at ng/L levels in urine, so a LOD at low ng/L is desirable.
5. Inject into the flow cell the sample (unknown hGH concentration), wait until stabilization of the signal and measure the sensor response.
6. Estimate the concentration of hGH in the sample by interpolating the measured sensor response in the fitting curve.

3.7 Data Analysis

To quantify the concentration of the target analyte in the sample, the sensor response is interpolated into the calibration curve. In order to minimize the estimation error and obtain accurate concentration values it is extremely important to employ an appropriate curve-fitting model. The most frequently model used to analyse immunoassay data is the 4-parameter logistic (4-PL) model, which fit the data by using the equation:

$$y = A_{\min} + \frac{(A_{\max} - A_{\min})}{1 + \left(\frac{x}{c}\right)^{b}}$$

where y is the sensor response, x is the concentration of the target analyte, $A_{\max}$ and $A_{\min}$ are the asymptotic ends, b is the slope at the inflection point of the curve and c is the concentration at the inflection point and represents the half maximal inhibitory concentration (IC_{50}) and the half maximal effective concentration (EC_{50}) in a competitive and a direct assay, respectively [13] (*see* **Note 10**). Typically, the detection limit (LOD) for a competitive and a direct assay is calculated as the analyte concentration for which the signal is inhibited or increase by 10% of sensor signal range ($A_{\max} - A_{\min}$), respectively, and the dynamic range (DR) of the biosensor is evaluated as the analyte concentrations that produced a sensor signal between 20 and 80% of ($A_{\max} - A_{\min}$) (*see* Fig. 4).

4 Notes

1. Polymer-based biosensors are increasingly popular, but the instability of the polymers, especially when they are in contact with a buffer solution, restricts their use. Progress in polymer material research could bring about advances in polymer-based IO biosensors in the near future.
2. EDC is hygroscopic and quickly oxidizes in air. A good way to handle EDC is to open the container under a dry inert

atmosphere such as nitrogen (e.g., inside a glovebox), separate it into aliquots, using containers which provide a tight seal, and then store aliquots at −20 °C. EDC solution must be prepared immediately before use.

3. Concentrated hydrochloric acid is corrosive and releases acidic gas. Therefore, handling of hydrochloric acid under a fume hood for approved acids and the use of personal protective equipment is strongly recommended.
4. Oxygen plasma treatment can be replaced by UV/Ozone plasma treatment (UV/Ozone ProCleaner™, Biorforce Nanosciences) for 1 h. Both oxidative pretreatments render highly hydrophilic surfaces (water contact angle lower than 5°). However, we recommend oxygen plasma rather than UV/Ozone plasma treatment, since it is less time-consuming and, in our experience, leads to surfaces with a slightly lower roughness.
5. Prevention of nonspecific adsorptions of sample matrix components is particularly important when working with label-free optical transducers in which an overvalued sensor response due to nonspecific adsorption of matrix components is difficult to discriminate and leads to false positive (direct immunoassay) or false negative (competitive immunoassay) results.
6. Alternately, adjust the flow rate to a value that keeps the injected sample volume in contact with the sensor surface during at least 1 h. Thus flow rates in the range of 2.0–2.5 and 3.5–4 μL/min are recommended for sample volumes of 150 and 250 μL, respectively.
7. The regeneration procedure depends on the antigen/antibody pair used. The ideal regeneration buffer should effectively disrupt the antigen-antibody interaction preserving the receptor activity. In practice, all regeneration buffers cause some damage on the bio-layer immobilized onto the transducer, limiting the number of cycles that the same sensor surface can be reused. Usually, either low pH (0.01–1 M HCl, 1–20% formic acid, 0.01–1 M phosphoric acid) or high pH (10–100 mM, 0.2 M Na_2CO_3) solutions, alone or in combination with chelating and surfactant reagents, are employed. Less but also employed are solutions of high ionic strength (1 M NaCl, 2–4 M $MgCl_2$) or chaotropic agents (8 M urea, 6 M guanidinium chloride), and nonpolar water-diluted solvents (20% acetonitrile, 10–100% ethanol). For high-affinity interactions, the used of a cocktail of different regeneration solutions may be necessary [14].
8. Antibody concentration has a strong effect on the sensitivity of the immunoassay and must be carefully optimized. In competitive immunoassays it is an advantage to use a low

concentration of the antibody since by decreasing antibody concentration the effect of the competitor (target analyte) is magnified, usually leading to a lower limit of detection (higher sensitivity). However, extremely low concentrations of antibody give a poor signal-to-noise ratio. Thus, a concentration leading to a response around 70% of that at the saturation limit is usually selected.

9. For fitting purposes, several data analysis and graphing software products such as SigmaPlot, OriginPro, or GraphPad Prism can be use.
10. 4-PL model gives rise to symmetric curves about the c point. If the experimental data rise to asymmetric curve, more complex functions, such as a five parameter logistic model, must be adopted [15, 16].

Acknowledgments

The nanoB2A is a consolidated research group (Grup de Recerca) of the Generalitat de Catalunya and has support from the Departament d'Universitats, Recerca i Societat de la Informació de la Generalitat de Catalunya (2014 SGR 624). ICN2 is the recipient of Grant SEV-2013-0295 from the "Severo Ochoa Centers of Excellence" Program of Spanish MINECO. The authors acknowledge to the European Union (BRAAVOO Grant Agreement No 614010). The authors thank Dr. Parlow (NIDDK, CA, USA), Dr. Rodríguez-Frade and Dr. M. Mellado (CNB-CSIC, Madrid, Spain), and Prof. Marco (IQAC-CSIC, Barcelona, Spain) for the supply of the inmunoreagents.

References

1. Hunsperguer RG (2009) Integrated optics: theory and technology. Springer, New York, NY
2. Nishihara H, Haruna M, Suhara T (1989) Optical integrated circuits, McGraw-Hill Optical and Electro-optical Engineering. Series, London
3. Kozma P, Kehl F, Ehrentreich-Förster E, Stamm C, Bier FF (2014) Integrated planar optical waveguide interferometer biosensors: A comparative review. Biosens Bioelectron 58:287–307
4. Zinoviev KE, González-Guerrero AB, Domínguez C, Lechuga LM (2011) Integrated bimodal waveguide interferometric biosensor for label-free analysis. J Light Technol 29:1926–1930
5. Mellado M, Rodriguez-Frade JM, Kremer L, Martinez-Alonso C (1996) Characterization of monoclonal antibodies specific for the human growth hormone 22 K and 20 K isoforms. J Clin Endocrinol Metab 81:1613–1618
6. Ballesteros, B., Barceló, D., Sanchez-Baeza, F., Camps, F. and Marco, M.P (1998) Influence of the Hapten Design on the Development of a Competitive ELISA for the Determination of the Antifouling Agent Irgarol 1051 at Trace Levels. Anal Chem 70, 4004–4014.
7. Ali, H.R, Arifin, M.M., Sheikh, M.A., Shazili, N.A.M. and Bachok, Z. (2013) Occurrence and distribution of antifouling biocide Irgarol-1051 in coastal waters of Peninsular Malaysia. Mar Pollut Bull 70, 253–257.
8. Martínez K, Ferrer I, Hernando MD, Fernández-Alba AR, Marcé RM, Borrull F, Barceló D (2001) Occurrence of Antifouling Biocides in

the Spanish Mediterranean Marine Environment. Environ Technol 22:543–552

9. Prieto F, Sepúlveda B, Calle A, Llobera A, Domínguez C, Abad A, Montoya A, Lechuga LM (2003) An integrated optical interferometric nanodevice based on silicon technology for biosensor applications. Nanotechnology 14:907–912
10. Dante S, Duval D, Fariña D, González-Guerrero AB, Lechuga LM (2015) Linear readout of integrated interferometric biosensors using a periodic wavelength modulation. Laser Photon Rev 9:248–255
11. Gandhiraman RP, Gubala V, Nam LCH, Volcke C, Doyle C, James B, Daniels S, Williams DE (2010) Deposition of chemically reactive and repellent sites on biosensor chips for reduced non-specific binding. Colloids Surfaces B 79:270–275
12. Peñalver A, Pocurull E, Borrull F, Marcé RM (1999) Solid-phase microextraction of the antifouling Irgarol 1051 and the fungicides dichlofluanid and 4-chloro-3-methylphenol in water samples. J Chromatogr A 839: 253–260
13. Dunn J, Wild D (2013) Calibration curve fitting. In: Wild D (ed) The immunoassay handbook, 4th edn. Elsevier, Oxford, pp 323–336
14. Fisher MJE (2010) Amine coupling through EDC/NHS: a practical approach. In: Mol NJ, Fischer MJE (eds) Surface Plasmon Resonance Methods and Protocols, 1st edn. Humana Press, Springer New York, pp 55–73
15. Gottschalk PG, Dunn JR (2005) The five-parameter logistic: a characterization and comparison with the four-parameter logistic. Anal Bioanal 343:54–65
16. Giraldo J, Vivas NM, Vila E, Badia A (2002) Assessing the (a)symmetry of concentration-effect curves: empirical versus mechanistic models. Pharmacol Ther 95:21–45